ACS APPLIED MATERIALS & INTERFACES

Research Article

www.acsami.org

Interface Engineering to Enhance the Efficiency of Conventional Polymer Solar Cells by Alcohol-/Water-Soluble C_{60} Materials Doped with Alkali Carbonates

Yu-Ying Lai, Ping-I Shih, Yi-Peng Li, Che-En Tsai, Jhong-Sian Wu, Yen-Ju Cheng,* and Chain-Shu Hsu*

Department of Applied Chemistry, National Chiao Tung University, 1001 Ta Hsueh Road Hsin-Chu, 30010, Taiwan

Supporting Information

ABSTRACT: Two new C_{60}-based n-type materials, **EGMC−OH** and **EGMC−COOH**, functionalized with hydrophilic triethylene glycol groups (TEGs), have been synthesized and employed in conventional polymer solar cells. With the assistance of the TEG-based surfactant, **EGMC−OH** and **EGMC−COOH** can be dissolved in highly polar solvents to implement the polar/nonpolar orthogonal solvent strategy, forming an electron modification layer (EML) without eroding the underlying active layer. Multilayer conventional solar cells on the basis of ITO/PEDOT:PSS/P3HT:PC_{61}BM/EML/Ca/Al configuration with the insertion of the **EGMC−OH** and **EGMC−COOH** EML between the active layer and the electrode have thus been successfully realized by cost-effective solution processing techniques. Moreover, the electron conductivity of the EML can be improved by incorporating alkali carbonates into the **EGMC−COOH** EML. Compared to the pristine device with a PCE of 3.61%, the devices modified by the Li_2CO_3-doped **EGMC−COOH** EML achieved a highest PCE of 4.29%. Furthermore, we demonstrated that the formation of the **EGMC−COOH** EML can be utilized as a general approach in the fabrication of highly efficient multilayer conventional devices. With the incorporation of the **EGMC−COOH** doped with 40 wt % Li_2CO_3, the **PCDCTBT−C8**:PC_{71}BM-based device exhibited a superior PCE of 4.51%, which outperformed the corresponding nonmodified device with a PCE of 3.63%.

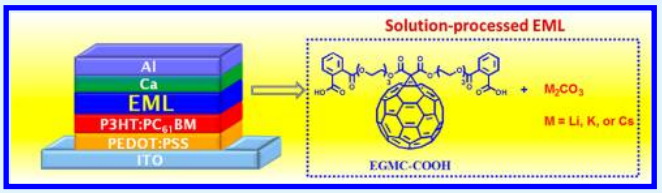

KEYWORDS: *polymer solar cells, interface engineering, hydrophilic fullerene materials, electron-selective layer, dopant, alkali carbonates*

INTRODUCTION

Bulk heterojunction (BHJ) solar cells based on polymer/fullerene blends have attracted enormous attention in the past decades due to their potential for fabrication onto large areas of lightweight and flexible substrates by low-cost solution processing.[1] A conventional BHJ polymer solar cell (PSC) with an active layer sandwiched by a low-work-function aluminum cathode and a hole-conducting poly(3,4-ethylenedioxylenethiophene):poly(styrenesulfonic acid) (PEDOT:PSS) layer on top of an indium tin oxide (ITO) substrate is the most widely used and researched device configuration.[2] By reversing the polarity of charge collection in the conventional cell, air-stable Ag can substitute for air-sensitive Al as the anodic electrode to construct a PSC with an inverted configuration.[3] In addition to development of p-type/n-type photoactive materials and control of nanomorphology,[4] interface engineering of multilayer conventional and inverted solar cells plays a critical role in achieving high efficiency and stability.[5] One of the directions of interfacial engineering is focused on the incorporation of an electron-selective layer, such as ZnO,[6] TiO_x,[7] LiF,[8] Cs_2CO_3,[9] poly(ethylene oxide),[10] and conjugated polyelectrolytes[11] between the active layer and the metal cathode for modulating the energy level alignment at the electrode/active layer interface, inducing electron-extracting/hole-blocking abilities, and facilitating electron transportation. Fullerene-based materials, in particular, emerge as the most superior n-type components to construct an electron-selective modification layer (EML) because their physical and electrical properties can be tailored and manipulated by attaching various addends on the core of fullerene.[12] For example, the fluorinated fullerene with the lower surface energy tends to self-assemble on the surface of the active layer during spin-coating to enhance the device performance.[12a,b] More importantly, the functional groups incorporated into C_{60} molecules can be specifically designed for fulfilling the processing requirements. For PSCs, multilayer structures are fabricated by layer-by-layer cost-effective spin-coating. One of the encountered challenges for solution processing techniques is the erosion of the bottom layer caused by organic solvents used in the subsequent step.[12g,h,13] For inverted PSCs, a solution of active layer needs to be deposited on top of a fullerene-based EML. Therefore, the development of chemically self-assembled[12c,d] and/or cross-linked fullerene materials[12e−h] to generate a robust and solvent-resistant EML has overcome the processing difficulties and thus successfully improved the device characteristics. With opposite sequence in a conventional device, however, a fullerene-based

Received: March 18, 2013
Accepted: May 20, 2013
Published: May 20, 2013

   dx.doi.org/10.1021/am400962e | ACS Appl. Mater. Interfaces 2013, 5, 5122−5128

Scheme 1. Synthesis of EGMC−OH and EGMC−COOH and the Structure of PCDCTBT−C8

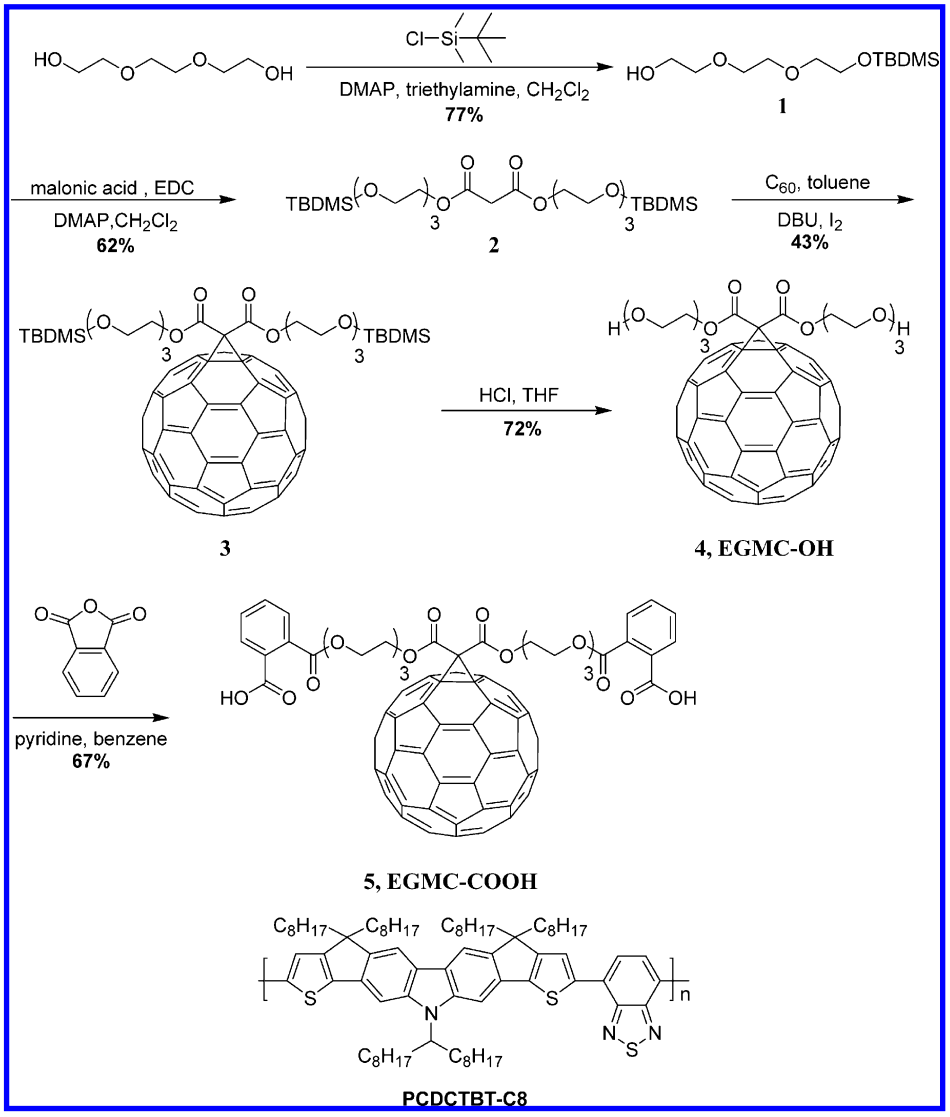

EML should be formed by spin-coating on top of the active layer. Considering that hydrophobic active layers such as P3HT/$PC_{61}BM$ are soluble in nonpolar organic solvents but almost insoluble in highly polar solvents, utilization of orthogonal solvents (i.e., nonpolar/polar) to construct multiple organic layers is a straightforward and practical strategy.[14] In this research, we have designed and synthesized two fullerene materials, **EGMC−OH** and **EGMC−COOH** (Scheme 1), containing hydrophilic triethylene glycol side chains. The two hydroxyl groups in **EGMC−OH** are further end-capped by two phthalic acids to yield **EGMC−COOH**. With the aid of triethylene glycol group (TEG)-based neutral surfactants, these C_{60} materials with enhanced hydrophilic nature can be dissolved in the polar 2-ethoxyethanol/H_2O solvent which was spin-cast to form an EML without destroying the underneath active layer. Therefore, we can successfully intercalate an EML between the active layer and the Ca/Al electrode in a conventional device. It has been demonstrated that the electron-transporting properties of organic semiconductors can be dramatically enhanced by adding alkali carbonates as n-dopants.[15] Alkali carbonates are ionic and highly polar compounds that can only be soluble in water. An organic active layer, such as P3HT/$PC_{61}BM$, is not compatible with the ionic or highly polar compounds. Therefore, the attempt of spin-coating pure alkali carbonates in aqueous solution on top of the organic active layer is not successful. Thermal vacuum coevaporation is the typical way to generate a thin film containing an alkali carbonate guest in a host material.[15a,b,d,g,h] Encouragingly, by the combination of water-/alcohol-soluble **EGMC−OH** and **EGMC−COOH** as the host materials with water-soluble alkali carbonates as the dopants, an n-doped C_{60}-based EML can be easily generated by cost-effective spin-coating processing. The P3HT:$PC_{61}BM$-based and poly(carbazole-dicyclopentathiophene-*alt*-benzothiadiazole) (**PCDCTBT−C8**, Scheme 1):$PC_{71}BM$-based devices integrating alkali carbonate-doped **EGMC−COOH** as the EMLs exhibited 19% and 24% improvement in efficiency, respectively, compared to their corresponding nonmodified cells.

EXPERIMENTAL SECTION

All chemicals were obtained from commercial sources and used as received unless otherwise specified. Anhydrous tetrahydrofuran, toluene, and dichloromethane were obtained from an SD-300 solvent purification system by AsiaWong Enterprise. NMR measurements are reported for Varian Unity-300 and UI-500 spectrometers (^1H, 300

dx.doi.org/10.1021/am400962e | ACS Appl. Mater. Interfaces 2013, 5, 5122−5128

MHz; ^{13}C, 75 MHz). Chemical shifts (δ values) are reported in parts per million with respect to Me_4Si (δ = 0 ppm) for ^{13}C and ^{1}H NMR. Coupling constants (J) are given in Hertz. ^{13}C NMR was proton broad-band-decoupled. Multiplicities of peaks are denoted by the following abbreviations: s, singlet; d, doublet; t, triplet; m, multiplet; br, broad. Thermogravimetric analysis (TGA) was recorded on a PerkinElmer Pyris analyzer under nitrogen atmosphere at a heating rate of 10 °C min^{-1}. Absorption spectra were collected on a HP8453 UV−vis spectrophotometer. Electrochemical cyclic voltammetry (CV) was conducted on a CH Instrument model 611D analyzer. Pt coated with a thin fullerene film was used as the working electrode, Ag/Ag$^+$ electrode as the reference electrode, and Pt as the counter electrode, while 0.1 M tetrabutylammonium hexafluorophosphate in *o*-dichlorobenzene was the electrolyte. CV curves were calibrated using ferrocence as the standard, whose oxidation potential is set at −4.8 eV with respect to zero vacuum level. The HOMO energy levels were obtained from the equation HOMO = $-(E_{ox}{}^{onset} - E_{(ferrocene)}{}^{onset} + 4.8)$ eV. The LUMO levels were obtained from the equation LUMO = $-(E_{red}{}^{onset} - E_{(ferrocene)}{}^{onset} + 4.8)$ eV

Synthesis of Tri(ethylene glycol) *tert*-Butyldimethylsilyl Ether (1). To an anhydrous CH_2Cl_2 (100 mL) solution of triethylene glycol (49.56 g, 0.33 mol), 4-dimethylaminopyridine (1.613 g, 13 mmol), and triethylamine (6.68 g, 66 mmol) was added dropwise an anhydrous CH_2Cl_2 (25 mL) solution of *tert*-butyldimethylsilyl chloride (10 g, 66 mmol) via an addition funnel under nitrogen atmosphere. The mixture was stirred at room temperature for 3 h and extracted with $CH_2Cl_2/NH_4Cl_{(aq)}$ three times. The collected organic layer was dried over $MgSO_4$, filtered, and evaporated in vacuo. The resultant residue was then submitted to column chromatography on silica gel (ethyl acetate:hexane = 1:3, v/v) to give a transparent liquid (13.45 g, 77%): ^{1}H NMR ($CDCl_3$, 300 MHz) δ 0.04 (s, 6H, $Si(CH_3)_2$), 0.86 (s, 9H, $C(CH_3)_3$), 2.60 (br, 1H, OH), 3.53−3.77 (m, 12H, OCH_2); ^{13}C NMR ($CDCl_3$, 75 MHz) δ −5.3 (2C, $SiCH_3$), 18.4 (1C, Si−**C**(Me)$_3$), 25.9 (3C, (Si−C(**C**H$_3$)$_3$), 61.8 (1C, OCH_2), 62.7 (1C, OCH_2), 70.4 (1C, OCH_2), 70.7 (1C, OCH_2), 72.5 (1C, OCH_2), 72.7 (2C, OCH_2).

Synthesis of Bis(TBDMS-triethylene glycol)-malonate (2). To an anhydrous CH_2Cl_2 (50 mL) solution of malonic acid (1 g, 9.60 mmol), 4-dimethylaminopyridine (0.234 g, 1.914 mmol), and **1** (5.69 g, 21.5 mmol) was added 1-ethyl-3-(3-dimethylaminopropyl)-carbodiimide (4.128 g, 26.60 mmol). The mixture was stirred at room temperature under nitrogen atmosphere for 15 h, evaporated to remove CH_2Cl_2, and extracted with ethyl acetate/H_2O three times. The collected organic layer was dried over $MgSO_4$, filtered, and evaporated. The resultant residue was then purified by column chromatography on silica gel (ethyl acetae:hexane = 1:6, v/v) to furnish a transparent liquid (3.5 g, 62%): ^{1}H NMR ($CDCl_3$, 300 MHz) δ 0.03 (s, 12H, $Si(CH_3)_2$), 0.86 (s, 18H, Si−C$(CH_3)_3$), 3.42 (s, 2H, (O═C)CH_2(C═O)), 3.53 (t, J = 5.19 Hz, 4H, OCH_2), 3.62−3.63 (m, 8H, OCH_2), 3.69 (t, J = 4.8 Hz, 4H, OCH_2), 3.74 (t, J = 5.5 Hz, 4H, OCH_2), 4.27 (t, J = 4.2 Hz, 4H, ((O═C)OCH_2); ^{13}C NMR ($CDCl_3$, 75 MHz) δ −5.3 (4C, Si−$(CH_3)_2$), 18.3 (2C, (Si−**C**(Me)$_3$), 25.9 (6C, (Si−C(**C**H$_3$)$_3$), 41.2 (1C, (O═C)**C**H$_2$(C═O)), 62.7 (2C, OCH_2), 64.6 (2C, OCH_2), 68.8 (2C, OCH_2), 70.6 (2C, OCH_2), 70.7 (2C, OCH_2), 72.7 (2C, OCH_2), 166.5 (2C, C═O).

Synthesis of Bis(TBDMS-triethylene glycol)-malonate Fullerene (3). To an anhydrous toluene (270 mL) solution of C_{60} (0.3 g, 0.416 mmol) was added sequentially **2** (0.25 g, 0.419 mmol), I_2 (0.102 g, 0.402 mmol), and 1,8-diazabicyclo[5.4.0]undec-7-ene (0.159 g, 1.04 mmol). The reaction mixture was stirred for 20 h and then quenched with sodium thiosulfate aqueous solution. The organic layer was collected, evaporated, and purified by column chromatography on silica gel (toluene:methanol)[a] to give a crude product, which was then reprecipitated from toluene/methanol to afford a brown solid (0.24 g, 44%): ^{1}H NMR ($CDCl_3$, 300 MHz,) δ 0.06 (s, 12H, $Si(CH_3)_2$), 0.89 (s, 18H, Si−C$(CH_3)_3$), 3.55 (t, J = 5.4 Hz, 4H, OCH_2), 3.63−3.69 (m, 8H), 3.76 (t, J = 5.4 Hz, 4H, OCH_2), 3.88 (t, J = 4.5 Hz, 4H, OCH_2), 4.64 (t, J = 5.1 Hz, 4H, (O═C)OCH_2); ^{13}C NMR ($CDCl_3$, 75 MHz) δ −5.2 (4C, $Si(CH_3)_2$), 18.4 (2C, Si−**C**(Me)$_3$), 25.8 (6C, Si−C(**C**H$_3$)$_3$), 62.67, 66.2, 68.8, 70.7, 71.4, 72.7, 139.1, 140.9, 141.8, 142.2, 142.9, 143.0, 143.1, 143.9, 144.6, 144.7, 144.9, 145.2, 145.3, 163.5 (2C, CO). [a]Initially, only toluene was used as the eluent to remove pristine C_{60}. Afterward, the eluent was changed to toluene:methanol = 98:2, v/v for collecting crude product.

Synthesis of Bis(triethylene glycol) Malonate C_{60} (4). To a THF (10 mL) solution of **3** (0.1 g, 0.076 mmol) was slowly added HCl (2 N, 1 mL). The reaction mixture was stirred vigorously at room temperature under nitrogen atmosphere for 30 min. An amount of 50 mL of CH_2Cl_2 was added, and the mixture was then washed by saturated $NaHCO_{3(aq)}$ and H_2O several times. The organic layer was collected, dried over $MgSO_4$, evaporated, and purified by column chromatography on silica gel (CH_2Cl_2:methanol = 30:1, v/v). The collected residue was then reprecipitated from CH_2Cl_2/hexane to furnish a brown solid (60 mg, 72%): ^{1}H NMR ($CDCl_3$, 300 MHz) δ 3.02 (s, 2H, OH), 3.60−3.63 (m, 4H, OCH_2), 3.67−3.70 (m, 4H, OCH_2), 3.72−3.75 (m, 8H, OCH_2), 3.91 (t, J = 4.8 Hz, 4H, OCH_2), 4.67 (t, J = 4.8 Hz, 4H, O═C−OCH_2); ^{13}C NMR($CDCl_3$, 75 MHz) δ 61.7, 66.1, 68.7, 70.4, 70.7, 72.7, 139.1, 140.9, 141.8, 142.2, 142.9, 143.0, 143.1, 143.9, 144.6, 144.7, 144.9, 145.1, 145.2, 145.3, 163.5 (2C, CO); MS (FAB, $C_{75}H_{26}O_{10}{}^{+\bullet}$) calcd, 1086.1526; found, 1086.1520

Synthesis of Bis(triethylene glycol phthalic acid)-malonate C_{60} (5). A mixture of **4** (0.05 g, 0.046 mmol), phthalic anhydride (0.136 g, 0.92 mmol), and benzene (30 mL) was heated to the refluxing temperature, and 2.5 mL of pyridine was then added. The refluxing was continued for 20 h. The reaction mixture was evaporated and purified by column chromatography on silica gel (CH_2Cl_2:methanol = 30:1, v/v). The collected residue was then reprecipitated from CH_2Cl_2/methanol to furnish a brown solid (43 mg, 67%): ^{1}H NMR ($CDCl_3$, 300 MHz) δ 3.68−3.70 (m, 4H, OCH_2), 3.76 (t, J = 4.2 Hz, 4H, OCH_2), 3.82−3.83 (m, 4H, OCH_2), 4.02 (t, J = 3.9 Hz, 4H, OCH_2), 4.44−4.46 (m, 4H, (O═C)OCH_2), 4.72 (t, J = 4.5 Hz, 4H, (O═C)OCH_2), 7.52−7.55 (m, 4H), 7.74−7.76 (m, 4H); ^{13}C NMR ($CDCl_3$, 75 MHz) δ 64.7 (2C, OCH_2), 65.7 (2C, OCH_2), 68.8 (2C, OCH_2), 68.9 (2C, OCH_2), 69.7 (2C, OCH_2), 70.9 (2C, OCH_2), 71.3, 128.9, 129.3, 130.9, 131.3, 131.5, 132.8, 138.9, 140.9, 141.8, 142.2, 142.9, 143.0, 143.8, 144.5, 144.6, 144.9, 145.1, 145.2, 145.2, 163.4 (2C, CO), 167.6 (2C, CO), 169.8 (2C, CO). MS (HR-FAB, $C_{91}H_{34}O_{16}{}^{+\bullet}$) calcd, 1382.1847; found, 1382.1859.

Device Fabrication. An indium tin oxide (ITO)-coated glass substrate was ultrasonically washed by detergent, deionic water, acetone, and isopropanol sequentially for 15 min each and then cleaned by UV-ozone for another 15 min. PEDOT:PSS (Baytron PVP AI-4083) was filtered and spin-coated on a cleaned ITO-coated glass to produce a ca. 35 nm thick interlayer, which was then baked at 150 °C for 1 h. For active-layer fabrication, P3HT was mixed with $PC_{61}BM$ in 1:1 weight ratio, and **PCDCTBT-C8** was mixed with $PC_{71}BM$ in 1:3 weight ratio, respectively, in *o*-dichlorobenzene. The weight percent of P3HT:$PC_{61}BM$ in *o*-dichlorobenzene was 2 wt %, and that of PCDTCBT:$PC_{71}BM$ was 1 wt %. The individual solutions were heated and spin-coated on top of the PEDOT:PSS interlayer at 600 rpm. The resultant film was covered in a Petri dish to allow the solvent to slowly evaporate (solvent annealing) until the film was dried and then baked at 140 °C for 10 min (thermal annealing). **EGMC−OH** or **EGMC−COOH** (2 mg) was then dissolved in mixed solvents (200 mg) and doped with an inorganic salt in some of the tested devices. The fullerene mixture was sonicated for 20 min, filtrated via a PVDF filter (45 μm), and spin-coated on top of the active layer at 3000 rpm for 60 s to give an 8 nm thick film. The top electrode was then prepared by sequential thermal evaporation of Ca (35 nm) and Al (100 nm) at reduced pressure below 10^{-6} Torr to furnish the BHJ solar cell devices. All devices contain an active area of 0.04 cm^2, and the photovoltaic parameters were measured at room temperature under air atmosphere with a Xenon lamp coupled to an AM 1.5G solar filter (SAN-EIXES-301S solar simulator). J−V characteristics were recorded in a Keitheley 2400 Source Measurement Unit.

RESULTS AND DISCUSSION

The synthetic procedure for the hydrophilic C_{60} derivatives is described in Scheme 1. Triethylene glycol was treated with *tert*-

butyldimethylsilyl chloride (TBDMS-Cl) in the presence of 4-dimethylaminopyridine (DMAP) and triethylamine in dichloromethane to give tri(ethylene glycol) *tert*-butyldimethylsilyl ether **1**. Esterfication of malonic acid with **1** by using 1-ethyl-3-(3-dimethylaminopropyl)carbodiimide and a catalytic amount of DMAP yielded **2**. Bingel reaction of C_{60} with **2** in the presence of 1,8-diazabicyclo[5.4.0]undec-7-ene and I_2 led to the formation of bis(TBDMS-triethylene glycol)-malonate fullerene **3**. Desilylation of **3** with hydrochloric acid (2 M) furnished bis(triethylene glycol) malonate C_{60} (**EGMC−OH**, **4**) which was reacted with phthalic anhydride to afford bis(triethylene glycol phthalic acid)-malonate C_{60} (**EGMC−COOH**, **5**). Their identities are fully characterized by NMR spectroscopy and mass spectrometry.

The cyclic voltammograms of $PC_{61}BM$, **EGMC−OH**, and **EGMC−COOH** are shown in Figure 1 and summarized in

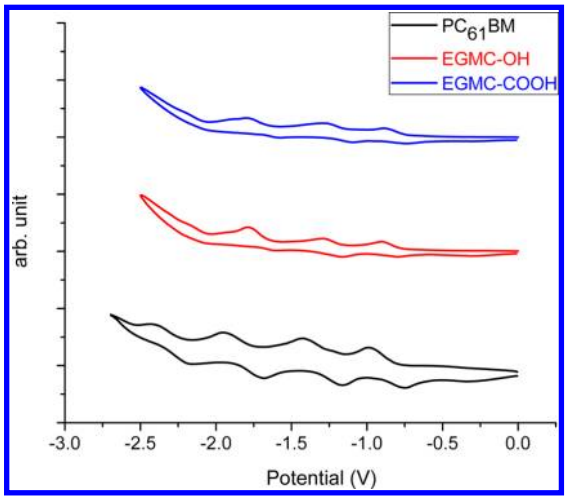

Figure 1. Cyclic voltammograms of $PC_{61}BM$ (black), **EGMC−OH** (red), and **EGMC−COOH** (blue).

Table 1. Redox Potential and LUMO Energy Levels for $PC_{61}BM$, EGMC−OH, and EGMC−COOH

compound	E^1pc^a(V)	E^1pa^b(V)	E^1red^c(V)	LUMO^d(eV)
EGMC−COOH	−0.886	−0.736	−0.811	−3.91
EGMC−OH	−0.910	−0.780	−0.845	−3.88
$PC_{61}BM$	−0.987	−0.752	−0.870	−3.85

[a]From the maximum of reduction potential. [b]From the maximum of oxidation potential. [c]From the equation $E_{red} = 0.5(E_{pc} + E_{pa})$. [d]From the equation LUMO = $-(4.72 + E_{red,onset})$.

Table 1. All voltammograms exhibit three well-defined, single-electron reversible waves in the scanning range. The LUMO energy levels of **EGMC−OH** (−3.88 eV) and **EGMC−COOH** (−3.91 eV) are both lower than that of $PC_{61}BM$ (−3.85 eV). The presence of the n-type EMLs can provide an extra donor−acceptor interface with the p-type material in the active layer for exciton dissociation. On the other hand, the intrinsically deep-lying HOMO energy level of **EGMC−OH** and **EGMC−COOH** effectively imparts the hole-blocking ability toward p-type material to reduce the charge recombination at the interfaces. The absorption spectra of **EGMC−OH** and **EGMC−COOH** are depicted in Figure 2. Both spectra are similar to each other with three distinct bands of ca. 258, 326, and 426 nm in the $CHCl_3$ solution.

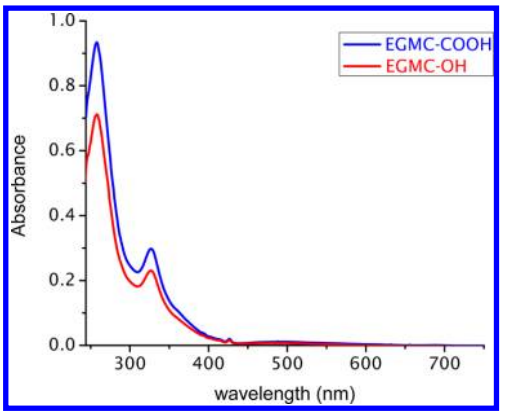

Figure 2. Absorption spectra of **EGMC−OH** (red) and **EGMC−COOH** (blue).

The strategy of using hydrophilic **EGMC−OH** and **EGMC−COOH** to construct the EML was then examined in conventional solar cells. The devices are fabricated on the basis of ITO/PEDOT:PSS/P3HT:$PC_{61}BM$/EML/Ca/Al configuration. The current density−voltage characteristics of the **EGMC−OH**-based devices are illustrated in Figure 3, and their

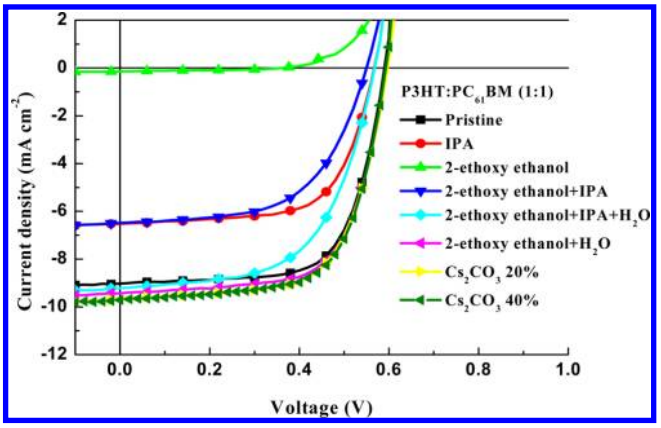

Figure 3. Current density−voltage characteristics of ITO/PEDOT:PSS/P3HT:$PC_{61}BM$/**EGMC−OH**/Ca/Al devices under illumination of AM1.5G at 100 mW cm^{-2}.

device parameters are summarized in Table 2. For comparison, the device without the EML was fabricated under otherwise identical conditions and yielded an open-circuit voltage (V_{oc}) of 0.6 V, a short-circuit current (J_{sc}) of 9.02 mA cm^{-2}, a fill factor (FF) of 67%, and a PCE of 3.61%. The choice of polar solvents for processing of the hydrophilic C_{60} plays an important role in determining the film-forming properties and the device characteristics, as shown in Table 2. Employing a less polar 2-ethoxyethanolfurnished a low PCE of 0.02%, while the device using isopropanol (IPA) as the solvent to deposit the **EGMC−OH** layer gave a PCE of 2.41%. Both 2-ethoxyethanoland isopropanol have a certain ability to dissolve $PC_{61}BM$ in the underlying active layer during the spin-coating of **EGMC−OH**, thus resulting in erosion and mixing of the active layer. The PCE was optimized to 3.71% when 2-ethoxylethanol/H_2O (10:1 v/v) was used as the processing cosolvent. The increased polarity as a result of H_2O strengthens the orthogonal solvent

dx.doi.org/10.1021/am400962e | ACS Appl. Mater. Interfaces 2013, 5, 5122−5128

Table 2. Photovoltaic Performances of the Devices Using EGMC−OH as the EML

solvent system	J_{sc} (mA cm^{-2})	V_{oc} (V)	FF (%)	PCE (%)	Rs (Ω*cm^2)	Rsh (Ω*cm^2)
no EML	9.02	0.60	67	3.61	10.00	603.0
IPA	6.52	0.56	66	2.41		
2-ethoxyethanol	0.14	0.36	38	0.02		
2-ethoxyethanol + IPA (5:1, v/v)	6.48	0.54	59	2.01		
2-ethoxyethanol + IPA + H_2O (5:5:1, v/v/v)	9.22	0.56	59	3.06		
2-ethoxyethanol + H_2O (10:1, v/v)	9.43	0.60	66	3.71	8.23	862.9

effect, thus forming the EML layer without altering the underlying active layer. Therefore, the formation of an **EGMC−OH**-based EML between the electrodes and the active layers enhanced the electron-transporting characteristics at the interfaces. A similar observation was found for the case of **EGMC−COOH**. The best efficiency of 3.80% was achieved when 2-ethoxylethanol/H_2O (10:1 v/v) was used as the cosolvent, indicating again the importance of utilizing highly polar solvents (Figure 4, Table 3). The devices with **EGMC−COOH** showed higher PCEs than those with **EGMC−OH**. These results may be presumably associated with the carboxylic acid functionality on **EGMC−COOH**. The two carboxylic groups might interact with the metal electrode and decrease the ohmic contact between the EML and the electrode, thus lowering the energy barrier for electron transporting from the EML to the electrode.[16] Furthermore, as can be concluded from Table 2 and Table 3, after the installation of the EML, the improvement of PCE mainly comes from the increase of J_{sc}, while the V_{oc} and FF values remained generally unchanged. The enhancement of J_{sc} is in resonance with the diminution of the device series resistance (Rs), indicating that the presence of the EML can improve the device conductivity.

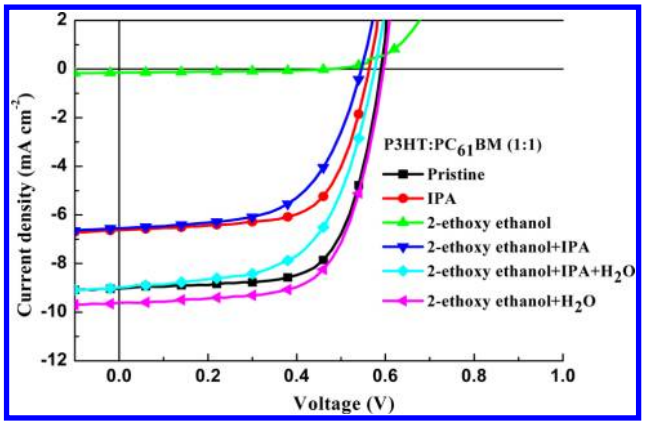

Figure 4. Current density−voltage characteristics of ITO/PEDOT:PSS/P3HT:$PC_{61}BM$/**EGMC−COOH**/Ca/Al devices under illumination of AM1.5G at 100 mW cm^{-2}.

In an attempt to further optimize the electron-transporting properties of the EML, n-dopant alkali carbonates were added into the **EGMC−OH** and **EGMC−COOH** hosts.[15a−d,g,h] Again, a 2-ethoxylethanol/H_2O (10:1, v/v) cosolvent system was used as the processing solvent for the following tests. As demonstrated in Table 4 and Figure 3, the device performance increased slightly upon the addition of Cs_2CO_3 in **EGMC−OH**-based EMLs. A PCE of 3.80% was achieved when 40 wt % Cs_2CO_3 was doped. The presence of Cs_2CO_3 can strengthen the electron-transporting ability of the EML by increasing the electron conductivity, thus resulting in the enhancement of J_{sc} and PCE. The doping effect is much more pronounced in the case of **EGMC−COOH**. An improved PCE of 4.21% was obtained as the doping content was increased to 40 wt % (Figure 5, Table 5). Encouraged by these results, we further evaluated different carbonates, i.e., Li_2CO_3 and K_2CO_3, which were incorporated in the **EGMC−COOH**-based EMLs as the n-dopants. As summarized in Figure 5 and Table 5, 40 wt % Li_2CO_3 is capable of increasing the J_{sc} from 9.61 mA cm^{-2} (without dopant) to 10.9 mA cm^{-2} and the PCE from 3.80% (without dopant) to 4.29%. Similar results can also be found for K_2CO_3 (Figure 5, Table 5). The significant improvement of PCE mainly comes from the increase of J_{sc}, while the V_{oc} and FF values remained generally unchanged. These results suggest again that alkali carbonates may enhance the conductivity of the EML, which is supported by comparing the conductivity of **EGMC−COOH** with and without doping of Cs_2CO_3 (see Figure S3 in the Supporting Information). Notably, this effect is more prominent in **EGMC−COOH** than **EGMC−OH**. The carboxylic acid groups of **EGMC−COOH** may interact with the carbonate bases from the ionic **EGMC**−carboxylate salt which is expected to have strong affinity with the metal

Table 4. Photovoltaic Performances of the Devices Incorporating EGMC−OH Doped with Cs_2CO_3

dopant	doping content in wt %[a]	J_{sc} (mA cm^{-2})	V_{oc} (V)	FF (%)	PCE (%)
no dopant	0%	9.43	0.60	66	3.71
Cs_2CO_3	20%	9.64	0.60	65	3.74
Cs_2CO_3	40%	9.71	0.60	65	3.80

[a]Wt % is the weight percentage of Cs_2CO_3 relative to **EGMC−OH**.

Table 3. Photovoltaic Performances of the Devices Incorporating EGMC−COOH as the EML

solvent system	J_{sc} (mA cm^{-2})	V_{oc} (V)	FF (%)	PCE (%)	Rs (Ω*cm^2)	Rsh (Ω*cm^2)
No EML	9.02	0.60	67	3.61	7.96	974.0
IPA	6.60	0.56	66	2.46		
2-ethoxyethanol	0.15	0.48	38	0.03		
2-ethoxyethanol + IPA (5:1, v/v)	6.54	0.54	60	2.12		
2-ethoxyethanol + IPA + H_2O (5:5:1, v/v/v)	8.98	0.58	60	3.10		
2-ethoxyethanol + H_2O (10:1, v/v)	9.61	0.60	66	3.80	7.19	1024.6

dx.doi.org/10.1021/am400962e | ACS Appl. Mater. Interfaces 2013, 5, 5122−5128

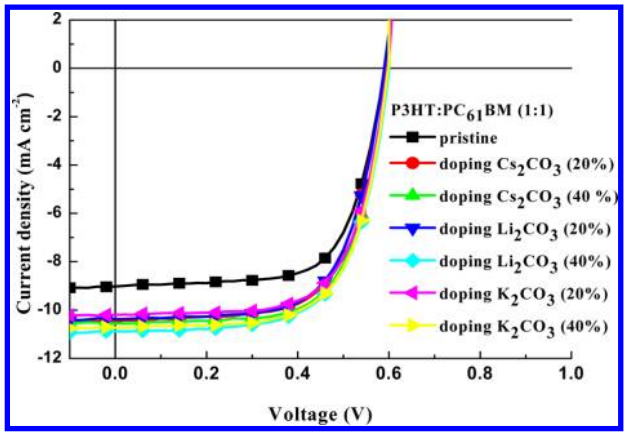

Figure 5. Current density–voltage characteristics of ITO/PEDOT:PSS/P3HT:$PC_{61}BM$/**EGMC–COOH**/Ca/Al devices doped with alkali carbonates.

electrode. The ohmic contact between the EML and the electrode is therefore reduced, leading to the enhancement of J_{sc} and PCE.[16]

To assess the applicability of the hydrophilic C_{60} materials doped with alkali carbonates as an EML, a low band polymer **PCDCTBT–C8** (Scheme 1) blended with $PC_{71}BM$ was then used as the active layer in a conventional device.[17] The reference device without the EML gave a V_{oc} of 0.72 V, a J_{sc} of 8.72 mA cm^{-2}, a FF of 57%, and a PCE of 3.63% (Table 6). The **PCDCTBT–C8**:$PC_{71}BM$-based device using **EGMC–COOH** as the EML doped with 40 wt % of Li_2CO_3 delivered a V_{oc} of 0.72 V, a J_{sc} of 11.1 mA cm^{-2}, a FF of 56%, and a PCE of 4.51%, which represents a 24% enhancement. Analogous to the P3HT:$PC_{61}BM$ system, the improvement of PCE mainly results from the increase of J_{sc}. This example demonstrates the general applicability of using alcohol-/water-soluble C_{60} materials for improving the efficiency of conventional solar cells.

CONCLUSIONS

We have rationally designed and synthesized two new C_{60}-based n-type materials, **EGMC–OH** and **EGMC–COOH**, functionalized with hydrophilic triethylene glycol groups. With the assistance of the TEG-based surfactant, **EGMC–OH** and **EGMC–COOH** can be dissolved in highly polar solvents to implement orthogonal solvent strategy, forming an electron modification layer without eroding the underlying active layer. We found that 2-ethoxylethanol/H_2O (10:1, v/v) with higher polarity is the best cosolvent to deposit the **EGMC–OH** and **EGMC–COOH** EMLs. Multilayer conventional solar cells (ITO/PEDOT:PSS/P3HT:$PC_{61}BM$/EML/Ca/Al) with insertion of the C_{60}-modifier between the active layer and electrode have been successfully realized by a cost-effective solution processing technique. Compared to the pristine device with a power conversion efficiency (PCE) of 3.61%, the device modified by the **EGMC–OH** and **EGMC–COOH** EMLs improved the PCEs to 3.71% and 3.8%, respectively. Moreover, the electron-transporting properties of **EGMC–OH** and **EGMC–COOH** can be further enhanced by the incorporation of alkali carbonates as the n-dopants. Regardless of the counterions, Cs_2CO_3, Li_2CO_3, as well as K_2CO_3 carbonates are all effective to obtain higher efficiency. The device using **EGMC–COOH** doped with 40 wt % Li_2CO_3 achieved a highest PCE of 4.29%. The superior performance of **EGMC–COOH** to **EGMC–OH** might be associated to the existence of the carboxylic functionality. Most importantly, the alcohol-/water-soluble **EGMC–COOH** can be applicable and effective to other conventional devices. With the incorporation of the **EGMC–COOH** EML doped with 40 wt % Li_2CO_3, the **PCDCTBT-C8**:$PC_{71}BM$-based device exhibited a superior PCE of 4.51%, which outperformed the corresponding nonmodified device with a PCE of 3.63%.

Table 6. Photovoltaic Performances of the PCDCTBT–C8:$PC_{71}BM$-Based Devices Using EGMC–COOH Doped with 40 wt % Li_2CO_3 as the EML

device	J_{sc} (mA cm^{-2})	V_{oc} (V)	FF (%)	PCE (%)
without EML	8.72	0.72	57	3.63
with EML	11.10	0.72	56	4.51

ASSOCIATED CONTENT

Supporting Information

Thermal gravimetric analysis, cyclic voltammograms, measurement of conductivity of **EGMC–COOH**, ^1H and ^{13}C NMR spectra, and mass spectrometry of the new materials. This material is available free of charge via the Internet at http://pubs.acs.org.

AUTHOR INFORMATION

Corresponding Author

*E-mail: yjcheng@mail.nctu.edu.tw and cshsu@mail.nctu.edu.tw.

Notes

The authors declare no competing financial interest.

ACKNOWLEDGMENTS

We thank the National Science Council and the "ATU Program" of the Ministry of Education and the Center for Interdisciplinary Science (CIS) of the National Chiao Tung University Taiwan for financial support.

Table 5. Photovoltaic Performances of the Devices Incorporating EGMC–COOH Doped with Alkali Carbonates

dopant	doping content in wt %[a]	J_{sc} (mA cm^{-2})	V_{oc} (V)	FF (%)	PCE (%)	Rs (Ω*cm^2)	Rsh (Ω*cm^2)
no dopant	0%	9.61	0.60	66	3.80	7.96	603.0
Cs_2CO_3	20%	10.5	0.60	65	4.09	7.61	2258.8
Cs_2CO_3	40%	10.6	0.60	66	4.21	7.19	2949.8
Li_2CO_3	20%	10.3	0.58	67	4.03	7.08	810.4
Li_2CO_3	40%	10.9	0.60	66	4.29	7.38	1220.9
K_2CO_3	20%	10.2	0.60	67	4.09	7.35	528.6
K_2CO_3	40%	10.7	0.60	67	4.28	7.05	640.5

[a]Wt % is the weight percentage of alkali carbonates relative to **EGMC–COOH**.

REFERENCES

(1) (a) Yu, G.; Gao, J.; Hummelen, J. C.; Wudl, F.; Heeger, A. J. *Science* **1995**, *270*, 1789−1791. (b) Günes, S.; Neugebauer, H.; Sariciftci, N. S. *Chem. Rev.* **2007**, *107*, 1324−1338. (c) Thompson, B. C.; Fréchet, J. M. J. *Angew. Chem., Int. Ed.* **2008**, *47*, 58−77. (d) Chen, J.; Cao, Y. *Acc. Chem. Res.* **2009**, *42*, 1709−1718. (e) Cheng, Y.-J.; Yang, S.-H.; Hsu, C.-S. *Chem. Rev.* **2009**, *109*, 5868−5923. (f) Zhou, H.; Yang, L.; You, W. *Macromolecules* **2012**, *45*, 607−632. (g) Li, Y.; Zou, Y. *Adv. Mater.* **2008**, *20*, 2952−2958. (h) Li, Y. *Acc. Chem. Res.* **2012**, *45*, 723−733.

(2) (a) Ma, W.; Yang, C.; Gong, X.; Lee, K.; Heeger, A. J. *Adv. Funct. Mater.* **2005**, *15*, 1617−1622. (b) Mayer, A. C.; Scully, S. R.; Hardin, B. E.; Rowell, M. W.; McGehee, M. D. *Mater. Today* **2007**, *10*, 28−33. (c) Li, G.; Shrotriya, V.; Huang, J.; Yao, Y.; Moriarty, T.; Emery, K.; Yang, Y. *Nat. Mater.* **2005**, *4*, 864−868. (d) Reyes-Reyes, M.; Kim, K.; Carroll, D. L. *Appl. Phys. Lett.* **2005**, *87*, 083506. (e) Woo, C. H.; Thompson, B. C.; Kim, B. J.; Toney, M. F.; Fréchet, J. M. J. *J. Am. Chem. Soc.* **2008**, *130*, 16324−16329.

(3) (a) Li, G.; Chu, C. W.; Shrotriya, V.; Huang, J.; Yang, Y. *Appl. Phys. Lett.* **2006**, *88*, 253503. (b) Liao, H.-H.; Chen, L.-M.; Xu, Z.; Li, G.; Yang, Y. *Appl. Phys. Lett.* **2008**, *92*, 173303. (c) Mor, G. K.; Shankar, K.; Paulose, M.; Varghese, O. K.; Grimes, C. A. *Appl. Phys. Lett.* **2007**, *91*, 152111. (d) Waldauf, C.; Morana, M.; Denk, P.; Schilinsky, P.; Coakley, K.; Choulis, S. A.; Brabec, C. J. *Appl. Phys. Lett.* **2006**, *89*, 233517. (e) White, M. S.; Olson, D. C.; Shaheen, S. E.; Kopidakis, N.; Ginley, D. S. *Appl. Phys. Lett.* **2006**, *89*, 143517. (f) Steim, R.; Choulis, S. A.; Schilinsky, P.; Brabec, C. J. *Appl. Phys. Lett.* **2008**, *92*, 093303. (g) Yang, T.; Cai, W.; Qin, D.; Wang, E.; Lan, L.; Gong, X.; Peng, J.; Cao, Y. *J. Phys. Chem. C* **2010**, *114*, 6849−6853.

(4) (a) Cheng, Y.-J.; Hsieh, C.-H.; Li, P.-J.; Hsu, C.-S. *Adv. Funct. Mater.* **2011**, *21*, 1723−1732. (b) Kim, B. J.; Miyamoto, Y.; Ma, B.; Fréchet, J. M. J. *Adv. Funct. Mater.* **2009**, *19*, 2273−2281. (c) Gholamkhass, B.; Holdcroft, S. *Chem. Mater.* **2010**, *22*, 5371−5376. (d) Drees, M.; Hoppe, H.; Winder, C.; Neugebauer, H.; Sariciftci, N. S.; Schwinger, W.; Schaeffler, F.; Topf, C.; Scharber, M. C.; Zhu, Z.; Gaudiana, R. *J. Mater. Chem.* **2005**, *15*, 5158−5163.

(5) (a) Li, C.-Z.; Yip, H.-L.; Jen, A. K.-Y. *J. Mater. Chem.* **2012**, *22*, 4161−4177. (b) Ma, H.; Yip, H.-L.; Huang, F.; Jen, A. K.-Y. *Adv. Funct. Mater.* **2010**, *20*, 1371−1388. (c) Yip, H.-L.; Jen, A. K.-Y. *Energy Environ. Sci* **2012**, *5*, 5994−6011. (d) Huang, F.; Jen, A. K.-Y. In *Organic Electronics*; CRC Press: Boca Raton, FL, 2009; pp 243−261.

(6) Hau, S. K.; Yip, H.-L.; Baek, N. S.; Zou, J.; O'Malley, K.; Jen, A. K. Y. *Appl. Phys. Lett.* **2008**, *92*, 253301.

(7) (a) Lee, K.; Kim, J. Y.; Park, S. H.; Kim, S. H.; Cho, S.; Heeger, A. J. *Adv. Mater.* **2007**, *19*, 2445−2449. (b) Gilot, J.; Wienk, M. M.; Janssen, R. A. J. *Appl. Phys. Lett.* **2007**, *90*, 143512. (c) Hayakawa, A.; Yoshikawa, O.; Fujieda, T.; Uehara, K.; Yoshikawa, S. *Appl. Phys. Lett.* **2007**, *90*, 163517.

(8) Brabec, C. J.; Shaheen, S. E.; Winder, C.; Sariciftci, N. S.; Denk, P. *Appl. Phys. Lett.* **2002**, *80*, 1288−1290.

(9) (a) Liao, H.-H.; Chen, L.-M.; Xu, Z.; Li, G.; Yang, Y. *Appl. Phys. Lett.* **2008**, *92*, 173303. (b) Chen, F.-C.; Wu, J.-L.; Yang, S. S.; Hsieh, K.-H.; Chen, W.-C. *J. Appl. Phys.* **2008**, *103*, 103721.

(10) (a) Zhang, F.; Ceder, M.; Inganäs, O. *Adv. Mater.* **2007**, *19*, 1835−1838. (b) Chen, F.-C.; Chien, S.-C. *J. Mater. Chem.* **2009**, *19*, 6865−6869.

(11) (a) Oh, S.-H.; Na, S.-I.; Jo, J.; Lim, B.; Vak, D.; Kim, D.-Y. *Adv. Funct. Mater.* **2010**, *20*, 1977−1983. (b) He, Z.; Zhang, C.; Xu, X.; Zhang, L.; Huang, L.; Chen, J.; Wu, H.; Cao, Y. *Adv. Mater.* **2011**, *23*, 3086−3089. (c) Luo, J.; Wu, H.; He, C.; Li, A.; Yang, W.; Cao, Y. *Appl. Phys. Lett.* **2009**, *95*, 043301. (d) Duarte, A.; Pu, K.-Y.; Liu, B.; Bazan, G. C. *Chem. Mater.* **2010**, *23*, 501−515. (e) He, C.; Zhong, C.; Wu, H.; Yang, R.; Yang, W.; Huang, F.; Bazan, G. C.; Cao, Y. *J. Mater. Chem.* **2010**, *20*, 2617−2622. (f) Seo, J. H.; Gutacker, A.; Sun, Y.; Wu, H.; Huang, F.; Cao, Y.; Scherf, U.; Heeger, A. J.; Bazan, G. C. *J. Am. Chem. Soc.* **2011**, *133*, 8416−8419. (g) He, Z.; Zhong, C.; Huang, X.; Wong, W.-Y.; Wu, H.; Chen, L.; Su, S.; Cao, Y. *Adv. Mater.* **2011**, *23*, 4636−4643. (h) He, Z.; Zhong, C.; Su, S.; Xu, M.; Wu, H.; Cao, Y. *Nature Photon.* **2012**, *6*, 591−595. (i) Duan, C.; Zhang, K.; Guan, X.; Zhong, C.; Xie, H.; Huang, F.; Chen, J.; Peng, J.; Cao, Y. *Chem. Sci.* **2013**, *4*, 1298−1307. (j) Guan, X.; Zhang, K.; Huang, F.; Bazan, G. C.; Cao, Y. *Adv. Funct. Mater.* **2012**, *22*, 2846−2854.

(12) (a) Wei, Q.; Nishizawa, T.; Tajima, K.; Hashimoto, K. *Adv. Mater.* **2008**, *20*, 2211−2216. (b) Jung, J. W.; Jo, J. W.; Jo, W. H. *Adv. Mater.* **2011**, *23*, 1782−1787. (c) Hau, S. K.; Cheng, Y.-J.; Yip, H.-L.; Zhang, Y.; Ma, H.; Jen, A. K. Y. *ACS Appl. Mater. Interfaces* **2010**, *2*, 1892−1902. (d) Duan, C.; Zhong, C.; Liu, C.; Huang, F.; Cao, Y. *Chem. Mater.* **2012**, *24*, 1682−1689. (e) Chang, C.-Y.; Wu, C.-E.; Chen, S.-Y.; Cui, C.; Cheng, Y.-J.; Hsu, C.-S.; Wang, Y.-L.; Li, Y. *Angew. Chem., Int. Ed.* **2011**, *50*, 9386−9390. (f) Cheng, Y.-J.; Hsieh, C.-H.; He, Y.; Hsu, C.-S.; Li, Y. *J. Am. Chem. Soc.* **2010**, *132*, 17381−17383. (g) Cheng, Y.-J.; Cao, F.-Y.; Lin, W.-C.; Chen, C.-H.; Hsieh, C.-H. *Chem. Mater.* **2011**, *23*, 1512−1518. (h) Hsieh, C.-H.; Cheng, Y.-J.; Li, P.-J.; Chen, C.-H.; Dubosc, M.; Liang, R.-M.; Hsu, C.-S. *J. Am. Chem. Soc.* **2010**, *132*, 4887−4893.

(13) (a) Cheng, Y.-J.; Liao, M.-H.; Shih, H.-M.; Shih, P.-I. *Macromolecules* **2011**, *44*, 5968−5976. (b) Huang, F.; Cheng, Y.-J.; Zhang, Y.; Liu, M. S.; Jen, A. K. Y. *J. Mater. Chem.* **2008**, *18*, 4495−4509. (c) Cheng, Y.-J.; Liu, M. S.; Zhang, Y.; Niu, Y.; Huang, F.; Ka, J.-W.; Yip, H.-L.; Tian, Y.; Jen, A. K. Y. *Chem. Mater.* **2007**, *20*, 413−422. (d) Müller, C. D.; Falcou, A.; Reckefuss, N.; Rojahn, M.; Wiederhirn, V.; Rudati, P.; Frohne, H.; Nuyken, O.; Becker, H.; Meerholz, K. *Nature* **2003**, *421*, 829−833.

(14) (a) Ayzner, A. L.; Tassone, C. J.; Tolbert, S. H.; Schwartz, B. J. *J. Phys. Chem. C* **2009**, *113*, 20050−20060. (b) Hagemann, O.; Bjerring, M.; Nielsen, N. C.; Krebs, F. C. *Sol. Energy Mater. Sol. Cells* **2008**, *92*, 1327−1335. (c) Zakhidov, A. A.; Lee, J.-K.; Fong, H. H.; DeFranco, J. A.; Chatzichristidi, M.; Taylor, P. G.; Ober, C. K.; Malliaras, G. G. *Adv. Mater.* **2008**, *20*, 3481−3484. (d) Sax, S.; Rugen-Penkalla, N.; Neuhold, A.; Schuh, S.; Zojer, E.; List, E. J. W.; Müllen, K. *Adv. Mater.* **2010**, *22*, 2087−2091.

(15) (a) Barbot, A.; Di, B. C.; Lucas, B.; Ratier, B.; Aldissi, M. *J. Mater. Sci.* **2013**, *48*, 2785−2789. (b) Xu, Z.-Q.; Yang, J.-P.; Sun, F.-Z.; Lee, S.-T.; Li, Y.-Q.; Tang, J.-X. *Org. Electron.* **2012**, *13*, 697−704. (c) He, M.; Jung, J.; Qiu, F.; Lin, Z. *J. Mater. Chem.* **2012**, *22*, 24254−24264. (d) Cai, Y.; Wei, H. X.; Li, J.; Bao, Q. Y.; Zhao, X.; Lee, S. T.; Li, Y. Q.; Tang, J. X. *Appl. Phys. Lett.* **2011**, *98*, 113304. (e) Huang, F.; Shih, P.-I.; Shu, C.-F.; Chi, Y.; Jen, A. K. Y. *Adv. Mater.* **2009**, *21*, 361−365. (f) Huang, F.; Shih, P.-I.; Liu, M. S.; Shu, C.-F.; Jen, A. K. Y. *Appl. Phys. Lett.* **2008**, *93*, 243302. (g) Wu, C.-I.; Lin, C.-T.; Chen, Y.-H.; Chen, M.-H.; Lu, Y.-J.; Wu, C.-C. *Appl. Phys. Lett.* **2006**, *88*, 152104. (h) Chen, S.-Y.; Chu, T.-Y.; Chen, J.-F.; Su, C.-Y.; Chen, C. H. *Appl. Phys. Lett.* **2006**, *89*, 053518.

(16) (a) O'Malley, K. M.; Li, C.-Z.; Yip, H.-L.; Jen, A. K. Y. *Adv. Energy Mater.* **2012**, *2*, 82−86. (b) Li, C.-Z.; Chueh, C.-C.; Yip, H.-L.; O'Malley, K. M.; Chen, W.-C.; Jen, A. K. Y. *J. Mater. Chem.* **2012**, *22*, 8574−8578.

(17) Cheng, Y.-J.; Wu, J.-S.; Shih, P.-I.; Chang, C.-Y.; Jwo, P.-C.; Kao, W.-S.; Hsu, C.-S. *Chem. Mater.* **2011**, *23*, 2361−2369.